Journal of Power Sources 363 (2017) 227–233

Contents lists available at ScienceDirect

Journal of Power Sources

journal homepage: www.elsevier.com/locate/jpowsour

# Effect of wettability-distribution pattern of the gas diffusion layer with a microgrooved separator on polymer electrolyte fuel cell performance

Yoshio Utaka [a, b, *], Ryo Koresawa [c]

[a] School of Mechanical Engineering, Tianjin University, No. 135 Yaguan Road, Tianjin Haihe Education Park, Tianjin 300350, China
[b] Key Laboratory of Efficient Utilization of Low and Medium Grade Energy (Tianjin University), Ministry of Education of China, China
[c] Graduate School of Engineering, Yokohama National University, 79-5 Tokiwadai, Hodogaya, Yokohama 240-8501, Japan

## HIGHLIGHTS

- Combination of hybrid GDL and microgrooves was examined for PEFC improvement.
- Effect of wettability pattern and aspect of GDL on PEFC performance was elucidated.
- Output characteristics were maximized at shallow hybrid angle with gas flow.

## ARTICLE INFO

*Article history:*
Received 23 May 2017
Received in revised form
11 July 2017
Accepted 25 July 2017

*Keywords:*
Polymer electrolyte fuel cell
Water management
Hybrid GDL
Wettability-distribution pattern
Gas channel
Microgrooves

## ABSTRACT

In this study, the combination of a gas diffusion layer (GDL) with wettability distribution and gas-flow channels with microgrooves is proposed to reduce the concentration overvoltage of polymer electrolyte fuel cells. The effects of the wettability-distribution pattern and linear angle of the stripe-wise wettability distribution of the GDL on the cell performance are experimentally investigated. Examination of the wettability-distribution pattern show that not only the liquid-water distribution inside a hybrid GDL but also the liquid-water control on the GDL surface are important factors to consider in reducing the concentration overvoltage. Furthermore, in considering the hybrid angle effect, when the angle with the gas channel is shallow, especially at 20°, the critical current and maximum power are maximized.



## 1. Introduction

Water management on the cathode side of polymer electrolyte fuel cells (PEFCs) is a dominant factor of the concentration overvoltage in determining the PEFC performance. The cell performance is greatly reduced by the excess water, which obstructs oxygen transport. Water management is critical for improving the performance of PEFC. Many studies have investigated the relationships among the structure and properties of the gas diffusion layer (GDL), microporous layer (MPL) and gas channel in the separator to improve moisture control and liquid water removal performance on the cathode side to control the water accumulation in a PEFC. The surface treatments of the GDL and the use of gas channels were examined. To cite a case, studies have considered using hydrophobic materials such as polytetrafluoroethylene (PTFE) for hydrophobic treatment of GDL [1–3]. The effects of a doublelayer GDL with different PTFE loadings [4] and PTFE content [5,6], and component fractions of hydrophobic and hydrophilic materials [7,8] for a MPL on cell performance have also been examined. Liquid water control using a GDL coated with an MPL containing hydrophilic carbon nanotubes [9], superhydrophobic MPL [10], multiple hydrophobic and hydrophilic MPLs [11] have also been developed. Concerning the gas channel in separator such as channel configuration have been examined for the effect on PEFC performance. Various flow channel types, such as parallel, serpentine,

* Corresponding author. School of Mechanical Engineering, Tianjin University, No. 135 Yaguan Road, Tianjin Haihe Education Park, Tianjin 300350, China.
*E-mail addresses:* utaka@ynu.ac.jp (Y. Utaka), koresawa-ryo-pr@ynu.jp (R. Koresawa).

http://dx.doi.org/10.1016/j.jpowsour.2017.07.095
0378-7753/

interdigitated, wettability of GDL surface have been investigated [12–20]. Other studies related to the configuration of the flow channel have considered sub-channel cathode flow field [21] and channel wall wettability [22,23]. Also, studies on water management and concentration-overvoltage characteristics were reviewed by Dai et al. [24], Kandlikar and Zijie [25], Kim and Lee [26], and Wang et al. [27].

We proposed that the function of novel oxygen diffusion based on the liquid-water movement from the non-wettable parts to the wettable parts due to the structure (hybrid GDL), which provides wettability distribution in the planar direction of the cathode side GDL of PEFCs, could be achieved. We demonstrated improved oxygen-diffusion characteristics in simulated microporous media that provide wettability distribution using equipment that measured the oxygen-diffusion characteristics (Utaka et al. [28]). Furthermore, we applied a carbon-paper-type hybrid GDL, where two porous media with different wettabilities (i.e., non-wettable and wettable) were alternately arranged in the planar direction, to a PEFC device and showed that improved PEFC performance was realized (Koresawa & Utaka [29]). Since liquid water was moved from the non-wettable medium to the wettable medium in hybrid GDL due to capillary pressure originating from the difference in wettability, voids in the non-wettable medium were aligned in the direction of oxygen diffusion, enhancing oxygen diffusion. While this wettability distribution in the GDL is effective for the liquid-water movement inside the GDL, limited amounts of liquid water can be removed from the GDL surface. To address this issue, we devised a mechanism to effectively remove liquid water from the GDL surface.

Inclined microgrooves were applied on the inner surfaces of gas channels in the separator. Liquid water was moved from the surface of the GDL to the opposing surface in the gas channel owing to the airflow shear forces that acted on the liquid water in the channel and the capillary forces that acted on the liquid water in the microgrooves. The flow velocity of the liquid water in the microgrooves was measured using the laser-induced fluorescence method. Liquid-water movement was confirmed to occur along a relatively long flow-path direction, demonstrating its effectiveness (Utaka et al. [30]). This microgroove design was also applied to an actual PEFC device to demonstrate improved PEFC performance (Koresawa & Utaka [31]). Additionally, a GDL with wettability distribution and a separator with microgrooves were installed at the same time (Utaka & Koresawa [32]) in an actual PEFC [29,31]. The combination of those two mechanisms is shown schematically in Fig. 1 [32]. An oxygen diffusion paths in the non-wettable area of

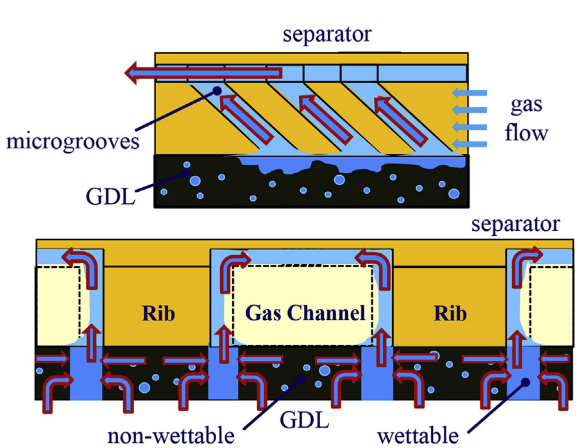


**Fig. 1.** Schematic of water movement with combination of hybrid GDL and microgrooves [32].

the GDL was ensured by the movement from non-wettable region to wettable region. Further, liquid water accumulated on the GDL surface in the wettable area was removed due to the mocrogroove effect. Those two functions of a hybrid GDL and a gas separator with microgrooves were combined and applied to an actual PEFC with an effective length of 200 mm [32]. Synergetic improvements in the PEFC performance were experimentally examined. As a result, the combination in PEFC reduced the concentration overvoltage and enhanced the current density limit and maximum power density compared with the normal PEFC, hybrid PEFC, and PEFC with microgrooves. At an air velocity of 8.0 m/s, the PEFC with microgrooves and a hybrid GDL improved the current density limit and maximum power density by approximately 19.5% and 8.0%, respectively, when compared with the normal PEFC. Moreover, the PEFC reduced the cell voltage fluctuation and improved the stability of the cell voltage due to an oxygen diffusion path formed by the movement of liquid water through the hybrid GDL and the discharge of liquid water from the GDL surface and the gas channels.

In a study related to the wettability distribution of GDLs, Forner-Cuenca et al. [33–35] applied a partial hydrophilic treatment to hydrophobic-paper-type GDLs in a small PEFC device; thus, a stripe-wise wettability-distribution pattern similar to that described by Utaka et al. [28] was achieved. Using neutron-beam visualization of liquid water, the effect of wettability distribution and improvement in power-generation characteristics were confirmed. Takaya and Araki [36] showed similar trends using numerical analyses for a compact PEFC with a striped GDL wettability distribution and microgrooves based on the experimental study of Utaka et al. However, because the generated water that accompanied the power generation increases in the downstream direction of the channel, control of the accumulated liquid water is extremely important. The effective length of the flow channel was as long as 200 mm in the previous experiments of Utaka et al. [29,31,32]. However, because the designed flow channels were targeted for small PEFCs with 10-mm channel effective lengths and a 1-$cm^2$ active area, examinations under actual PEFC conditions will be insufficient.

The effect of the pattern and arrangement of the GDL wettability distribution using actual PEFC equipment with a combined hybrid GDL and microgrooved separator channels were investigated in this study. In previous reports [29,32], the wettability-distribution pattern of alternately arranged wettable and non-wettable stripes had stripe widths of approximately 1 mm and stripe angles of 45° with the gas flow. However, because the generated water flow, which increased with the gas-channel length, and the configuration of the wettability distribution are closely related, the configuration of the wettability distribution affects the liquid-water distribution inside and outside the GDL. Therefore, the morphological effects of the wettability distribution with respect to the oxygen diffusion and PEFC output characteristics should be considered. In the present work, the relationship between the PEFC performance and basic control factors that regulate the output characteristics of PEFCs, such as cell temperature, air humidity, and configuration of the GDL wettability distribution, was examined. On the basis of these investigations, we then experimentally determined the effect of the angle between the linear GDL wettability distribution and gas-channel direction on the PEFC performance.

## 2. Experimental apparatus and procedure

A summary of the experimental conditions and PEFC specifications is listed in Table 1. The hydrogen supplied to the anode and the air (approximately 78% nitrogen, 21% oxygen, and 1% argon)

**Table 1**
Experimental conditions and specifications of the PEFC apparatus.

| | |
|---|---|
| Experimental conditions | |
| Active electrode area (geometric) ($cm^2$) | 2.1 × 20.0 |
| Clamping pressure (MPa) | 1.23 |
| Cell temperature (°C) | 50, 70, 80, and 90 |
| Relative humidity (%) | 20, 50, 70, and 100 |
| Gas velocity (flow rate) | |
| Hydrogen (m/s) (mL/min) | 1.2 (800) |
| Air (m/s) (mL/min) | 5.0 (3300)–15.0 (9900) |
| Specifications of GDL, MPL, and the separator | |
| Hybrid GDL (wettability-distribution pattern) | Linear (0°, 20°, 30°, and 45°), Grid (±45°) |
| MPL treatment (mg/$cm^2$) | Polytetrafluoroethylene: 2.0, Carbon: 2.0 |
| Flow field design | parallel |
| Gas-channel width (mm) | 1.0 |
| Gas-channel depth (mm) | 1.0 |
| Rib width (mm) | 1.0 |
| Inclination angle of microgrooves (°) | 20 |
| Width of microgrooves (mm) | 0.2 |
| Depth of microgrooves (mm) | 0.2 |

supplied to the cathode were provided from gas cylinders via humidifiers and mass-flow controllers set to constant flow rates. The supply gases were saturated at a predetermined temperature in the humidifiers.

To operate the PEFC main body at a predetermined temperature, temperature control was maintained by passing gases through constant-temperature water in a tank to the anode and cathode separators. The relative humidity of the supplied gas was also set.

Fig. 2 shows the configuration of the PEFC used in this study. The separator was made of gold-plated brass with a cooling water flow path, a current collector, inlet and outlet manifolds for the supply gas, and gas-flow channels (with parallel flow paths).

The size of the separator was 86 mm × 258 mm with parallel gas-flow passages in the central 21 mm × 200 mm part. Two types of flow channels, namely conventional and microgrooved channels, were used. A conventional flow channel with a rectangular cross section 1-mm wide and 1-mm deep and 11 flow channels, 200 mm long was installed. Ten ribs with a width of 1 mm and length of 200 mm were installed between the flow paths. The channel temperatures were measured using T-type sheath thermocouples installed in the thermocouple holes provided at six locations between the high-temperature water and gas-flow channels. Additionally, temperature-controlled water was passed through three 7-mm-diameter flow paths located at the center of the cell (18 mm from the left and right of the cell). The separators with microgrooves were also made of gold-plated brass. Except for the added microgrooves, these separators had the same basic structure and functions (i.e., cooling, current collection, and gas-flow path) as the conventional separators. Based on the results obtained by Utaka et al. [30], the details in Fig. 3 (a) show that the flow channels with microgrooves had an inclination angle of 20° and a width and depth of 0.2 mm, arranged at 0.2-mm intervals (i.e., a pitch of 0.4 mm perpendicular to the groove centerline). The separator with microgrooves was used only at the cathode where water production by power generation occurred. A conventional separator was used for the anode. The microgrooves in the separator were installed from 50 to 200 mm downstream of the flow channel where the flow rate of the generated liquid water increased.

A carbon-paper Toray TGP-H-060 GDL with a thickness of 190 μm and porosity of 78% coated with a microporous layer (MPL) on one side was used. Table 1 lists the details of the GDL. The size of the GDL was 21 mm × 200 mm, i.e., the same as the reaction area. The size of the polymer electrolyte membrane (PEM) was equal to that of the separator and was 86 mm × 258 mm. Catalyst layers were coated on both sides (corresponding to the anode and cathode) of the central part of a 21 mm × 200 mm PEM, which served as

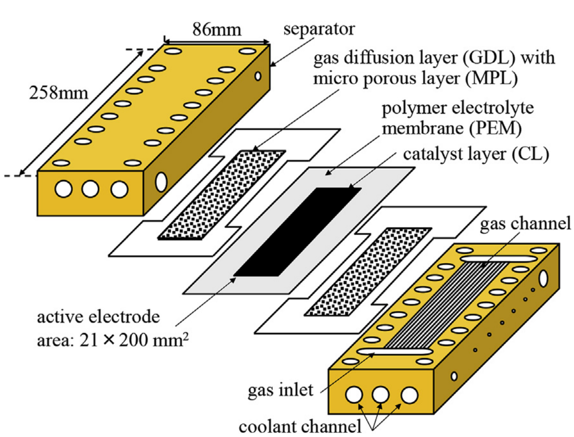


**Fig. 2.** Schematic of the PEFC components.

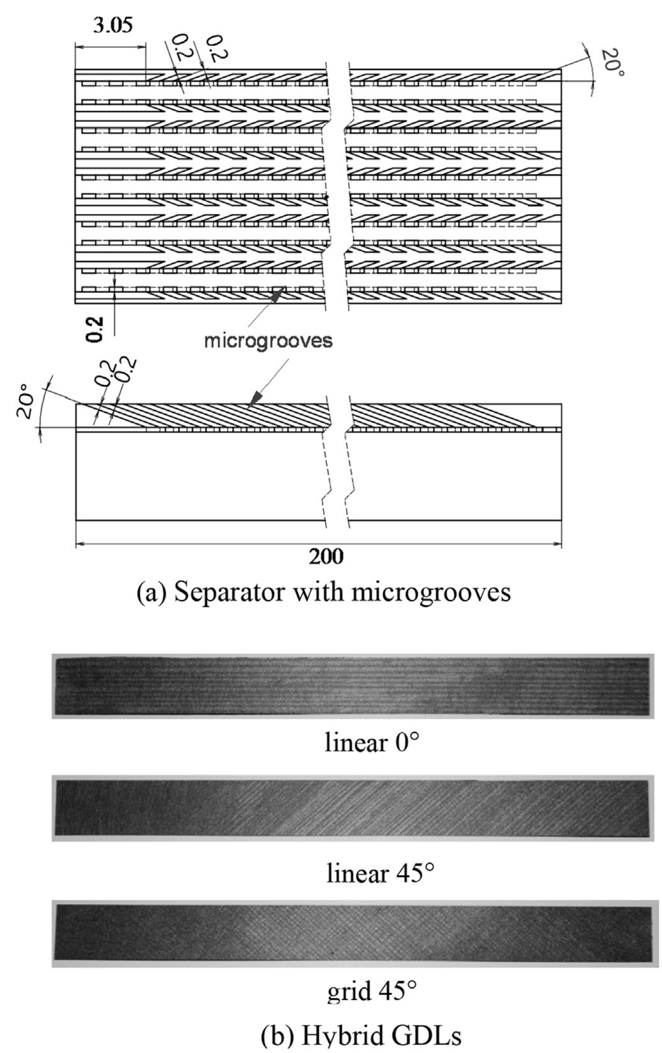


**Fig. 3.** Details of the separator with microgrooves and wettability-distribution pattern of the hybrid GDLs.

the position of the gas-flow channel of the separator.

A sample hybrid GDL is shown in Fig. 3 (b). Two hybrid GDLs with inclination angles of the linear non-wettable treated regions (i.e., linear angles) relative to the gas-flow direction were indicated to have angles of 0° and 45° (linear 0° and 45°). In addition, a hybrid GDL with −45° and +45° non-wettable treated stripes in a lattice pattern (i.e., grid 45°) is shown. The dark linear portions in the figure represent the areas subjected to non-wettable treatment. Hybrid GDLs with linear angles of 20° and 30° (linear 20° and 30°) were also used in the experiment. These configurations determined the characteristics of not only the liquid-water transfer inside the hybrid GDL but also the control of surface liquid water, which increased with the gas-flow path. For example, covering the non-wettable portion with liquid water may cause accumulation on the GDL surface due to the bridging the wettable portions by the liquid water. Therefore, the hybrid GDL has functions of prevention of bridging and supply of liquid water to the root of the microgrooves.

## 3. Experimental results and discussion

### 3.1. Effect of basic factors on the cell performance characteristics

Figs. 4 and 5 show the influence of cell temperature and air humidity, which are fundamental factors, when a linear 45° hybrid GDL is used. The results of the gas-flow channels with and without microgrooves are shown in each figure. Fig. 4 shows the current–voltage characteristics when the cell temperature was varied from 50 to 90 °C. As shown by Koresawa and Utaka [31], improvements in cell characteristics were observed after application of the microgrooves. Regardless of the presence or absence of microgrooves, better cell performance was observed at 70 and 80 °C.

Fig. 5 shows the current–voltage characteristics when the relative humidity of air and hydrogen gas at the inlets was varied from 20% to 100%. Compared to the influence of temperature, the effect of humidity was higher. Furthermore, a significant performance deterioration occurred, particularly in the low-humidity of 20% cases. Further voltage drop appeared after the microgrooves were added. This shows the negative effect on PEFC performance due to the liquid removal of microgrooves. In either case, it was shown that the use of PEFC at extremely low humidity condition is not favorable. At 50% and 70% humidity levels, relatively significant performance improvements were observed after the microgrooves were added. Because of the high levels of liquid water in the channel environment at these relatively high-humidity conditions, the addition of microgrooves significantly improved the cell

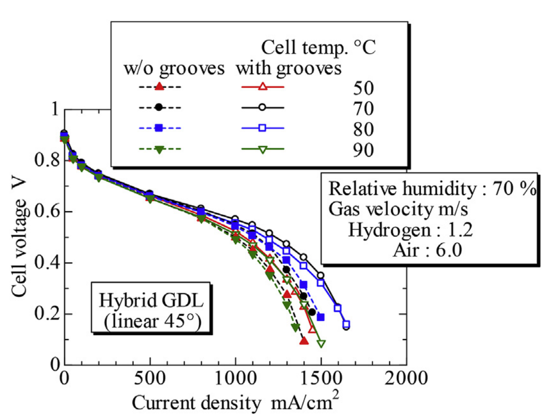


**Fig. 4.** Effect of the cell temperature as a basic parameter on the cell performance for cases with and without microgrooves.

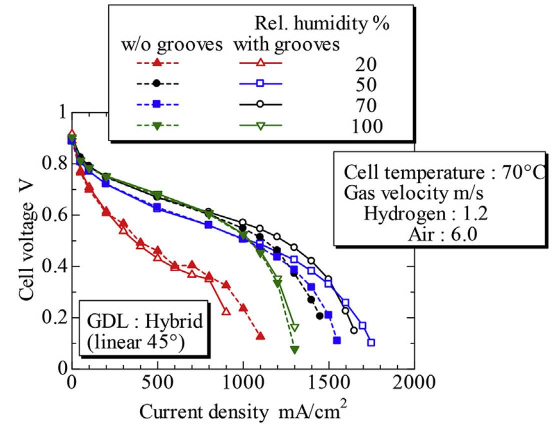


**Fig. 5.** Effect of relative humidity as a basic parameter on the cell performance for cases with and without microgrooves.

operation. However, at humidity conditions of 100%, PEFC performance decreased and the influence of the microgrooves became smaller.

Fig. 6 (a) and (b) shows the current–voltage characteristics of two PEFCs with two different hybrid GDL configurations of linear 45° and grid 45° for a ±45° stripe arrangement with and without microgrooves at air-flow velocities that varied from 5.0 to 8.0 m/s. Optimal cell performance was observed at approximately 70 °C and 70% cell temperature and inlet-gas relative humidity, respectively, as shown in Figs. 4 and 5. These parameters govern the PEFC characteristics, and these optimum values were used as standard references. The comparison of Fig. 6 (b) with Fig. 6 (a) revealed improvements in the cell after the microgroove application. The effects of the microgrooves on the air velocity were more pronounced. Although Fig. 6 (a) shows that the PEFC without microgrooves indicated an increase in the critical current density of approximately 200 mA/cm$^2$ when the airflow rate was varied from 5 to 8 m/s, a difference of more than two times the approximately 500 mA/cm$^2$ critical current density in the PEFC with microgrooves [Fig. 6] (b) was realized. This difference was closely related to the removal of liquid water by the microgrooves owing to the shear force caused by the air flow. In the absence of microgrooves, the difference in performance was relatively small. However, with the microgrooves, the critical current density increased as the air-flow velocity increased because the influence of the air-flow velocity increased.

The grid 45° configuration, when compared with the linear 45° configuration, was initially expected to improve the hybrid GDL performance because the moving ability of liquid water increased inside the GDL due to the increased wettability boundary length between the wetted and non-wetted parts. However, as shown by the experimental results, regardless of the presence of microgrooves, the performance of the grid 45° configuration remarkably decreased when compared with that of the linear 45° configuration. The difference in the cell performance was likely dependent on the positional relationship between the wettable part and the gas flow-path direction in the hybrid GDL because it depends on the drainage characteristics from the GDL surface in the gas channel. For the grid 45° GDL, the wettable part was surrounded by non-wettable parts. Depending on the positional relationship between the gas-flow path and the wettable part, liquid water accumulated at the wettable area, and the concentration overvoltage readily increased. For example, when wettable part was located at center of flow-channel, block off the channel may occurred. On the other hand, accumulation of water easily arose from wettable area

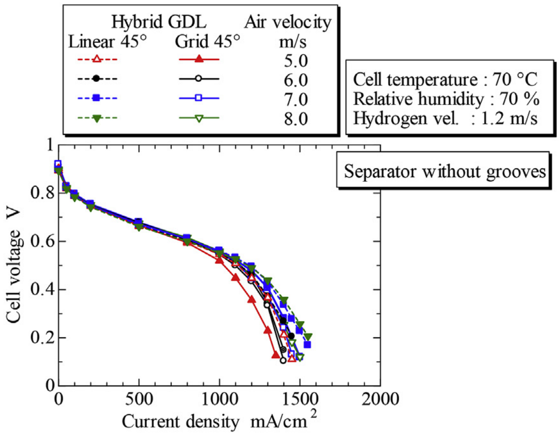


(a) I–V curves for hybrid GDL without microgrooves

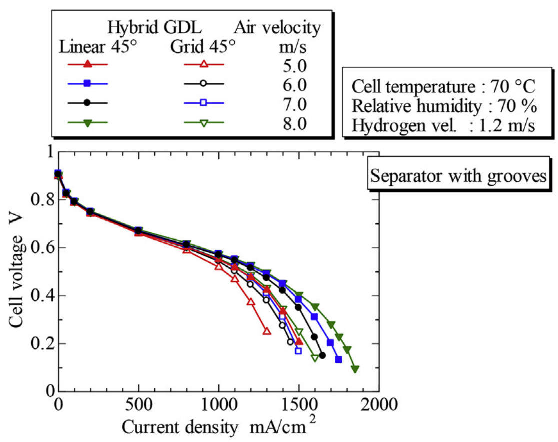


(b) I–V curves for hybrid GDL with microgrooves

**Fig. 6.** Comparison of the power generation characteristics between the hybrid GDLs of linear and grid patterns with and without microgrooves in gas channels.

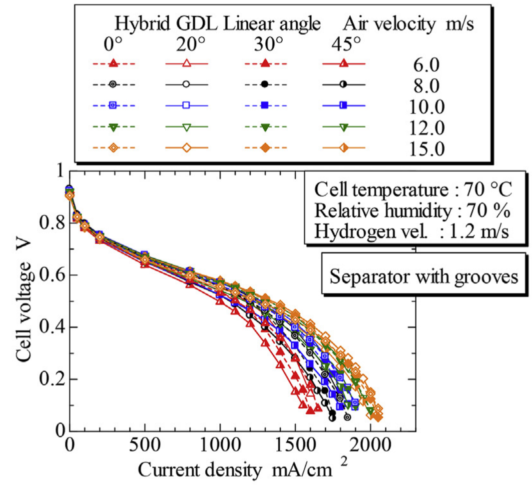


(a) I–V curves

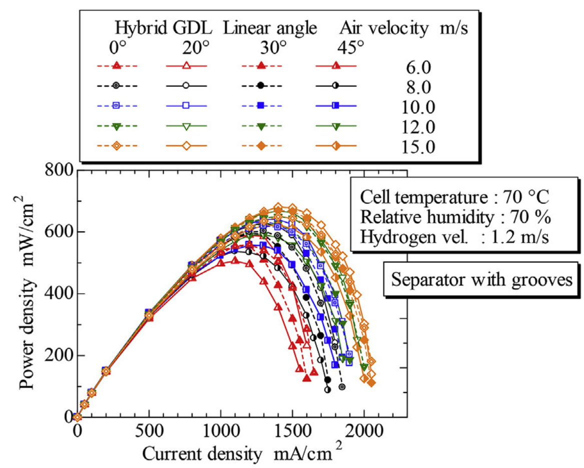


(b) Power density curves

**Fig. 7.** Effect of the linear angle of the wettability pattern distribution on the cell performance.

positioned under rib. As a result, an apparent power generation difference was observed.

Thus, as described above, for the hybrid GDL, not only the liquid-water movement inside the GDL but also the liquid-water accumulation on the GDL surface should be carefully controlled; consequently, the configuration of the wettability distribution is important.

### 3.2. *Effect of the installation angle of the linear wettability distribution in hybrid GDL*

Next, the effect of the linear angle of the wettability distribution relative to the gas-flow channel was examined. As mentioned earlier, we only measured the linear 45° configuration and considered this angle in exploring the liquid-water control on the GDL surface. Furthermore, the cell performance was investigated over a broad air-flow velocity range because of the remarkable dependence of the liquid-water behavior on the air flow and its response to larger air-flow rate to the channel, such as that in a serpentine configuration.

Fig. 7 shows the effect of the linear angle on the cell performance. Fig. 7 (a) and (b) shows the current density–voltage curves and the output density characteristic curves, respectively. The PEFC was configured with microgrooves, the cell temperature and air and hydrogen relative humidity were set to 70 °C and 70%, respectively, and the air-flow velocity range was expanded to 6.0–15.0 m/s. The linear angle was set to 0° for a parallel configuration with the gas channel, and angles of 0°, 20°, 30° and 45° were examined. From both figures, when the microgrooves and hybrid GDL were combined, noticeable performance improvements were observed due to the increased air-flow velocities. The effect of the hybrid angle was confirmed, and the cell performances for the linear 0°, 20°, and 30° was higher than that for linear 45°. In particular, the performance was the highest for the linear 0° and 20° configurations, which were relatively shallow angles relative to the liquid-water flow path. Because the configurations of the wettable and non-wettable parts were the same for all angles, control of the liquid-water accumulation on the GDL surface is important. At shallow angles, the influence of the surface covered by liquid water present in the wetted part on the upstream side of the non-wettable part appeared to have a smaller effect.

The critical current density and maximum output point are shown in Fig. 8 for each examined linear angle to determine the characteristics of the current density–voltage and output density curves. Here, the critical current density was defined at a voltage of 0.2 V. Among the four linear angles investigated (i.e., 0°, 20°, 30°,

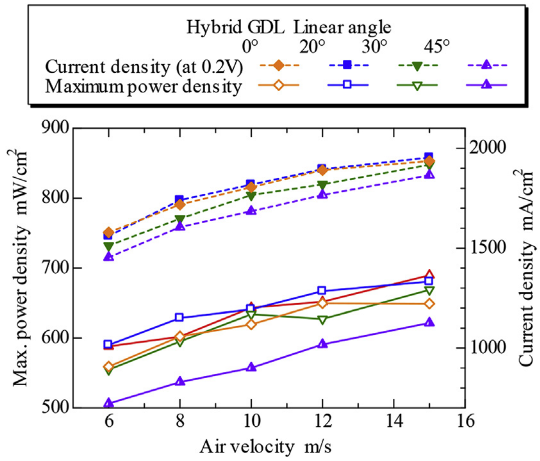


**Fig. 8.** Comparison of the effects of the linear angle on the wettability pattern on the cell performance.

and 45°), the performance was the highest at shallow angles of 0° and 20°, especially at 20°. Under these conditions, the PEFC performance was high over the entire range of studied air-flow velocity, and the maximum power and critical current density were maximized.

## 4. Conclusions

In this study, we have experimentally examined the influence of a hybrid pattern and hybrid angle using a PEFC by applying the hybrid GDL with a wettability-distribution pattern and gas channels with microgrooves. The following results were obtained:

(1) The effects of cell temperature and gas-inlet relative humidity, which are basic factors in fuel cells, were studied for the combined hybrid GDL with the wettability distribution and separator with microgrooves.
(2) Based on the relationship between the hybrid pattern and output characteristics of the fuel cell, liquid-water control on the GDL surface as well as liquid-water distribution inside the hybrid GDL are important factors to consider.
(3) The effect of the hybrid angle of the linear wettability-distribution pattern on the gas channel was presented. The hybrid angle should be shallow, preferably 20°, where the critical current density and maximum power are optimized.

## Acknowledgements

This work was supported in part by JSPS KAKENHI Grant Number 23360097 and in part by the Strategic International Collaborative Research Program of the Japan Science and Technology Agency.

## References

[1] G.G. Park, Y.J. Sohn, T.H. Yang, Y.G. Yoon, W.Y. Lee, C.S. Kim, Effect of PTFE contents in the gas diffusion media on the performance of PEMFC, J. Power Sources 131 (2004) 182–187.
[2] K.T. Cho, M.M. Mench, Effect of material properties on evaporative water removal from polymer electrolyte fuel cell diffusion media, J. Power Sources 195 (2010) 6748–6757.
[3] Z. Lu, C. Rath, G. Zhang, S.G. Kandlikar, Water management studies in PEM fuel cells, part IV: effects of channel surface wettability, geometry and orientation on the two-phase flow in parallel gas channels, Int. J. Hydrog. Energy 41 (2011) 9864–9875.
[4] Y. Wang, L. Wang, S.G. Advani, A.K. Prasad, Double-layer gas diffusion media for improved water management in polymer electrolyte membrane fuel cells, J. Power Sources 292 (2015) 39–48.
[5] Z. Qi, A. Kaufman, Improvement of water management by a microporous sublayer for PEM fuel cells, J. Power Sources 109 (2002) 38–46.
[6] H.K. Atiyeh, K. Karan, B. Peppley, A. Phoenix, E. Halliop, J. Pharoah, J. Power Sources 170 (2007) 111–121.
[7] S. Park, J.W. Lee, B.N. Popov, Effect of PTFE content in microporous layer on water management in PEM fuel cells, J. Power Sources 177 (2008) 457–463.
[8] G. Velayutham, Effect of micro-layer PTFE on the performance of PEM fuel cell electrodes, Int. J. Hydrog. Energy 36 (2011) 14845–14850.
[9] T. Kitahara, H. Nakajima, K. Okamura, Gas diffusion layers coated with a microporous layer containing hydrophilic carbon nanotubes for performance enhancement of polymer electrolyte fuel cells under both low and high humidity conditions, J. Power Sources 283 (2015) 115–124.
[10] S. Latorrata, P.G. Stampino, C. Cristiani, G. Dotelli, Novel superhydrophobic microporous layers for enhanced performance and efficient water management in PEM fuel cells, Int. J. Hydrog. Energy 39 (2014) 5350–5357.
[11] T. Kitahara, H. Nakajima, M. Inamoto, K. Shinto, Triple microporous layer coated gas diffusion layer for performance enhancement of polymer electrolyte fuel cells under both low and high humidity conditions, J. Power Sources 248 (2014) 1256–1263.
[12] T.V. Nguyen, A gas distributor design for proton-exchange-membrane fuel cells, J. Electrochem. Soc. 143 (1996) L103–L105.
[13] D.L. Wood III, J.S. Yi, T.V. Nguyen, Effect of direct liquid water injection and interdigitated flow field on the performance of proton exchange membrane fuel cells, Electrochim. Acta 43 (1998) 3795–3809.
[14] F.B. Weng, A. Su, C.Y. Hsu, C.Y. Lee, Study of water-flooding behaviour in cathode channel of a transparent proton-exchange membrane fuel cell, J. Power Sources 157 (2006) 674–680.
[15] S. Shimpalee, S. Greenway, J.W. Van Zee, The impact of channel path length on PEMFC flow-field design, J. Power Sources 160 (2006) 398–406.
[16] W.M. Yan, H.Y. Li, P.C. Chiu, Xiao-Dong Wang, Effects of serpentine flow field with outlet channel contraction on cell performance of proton exchange membrane fuel cells, J. Power Sources 178 (2008) 174–180.
[17] K.S. Choi, H.M. Kim, S.M. Moon, An experimental study on the enhancement of the water balance, electrochemical reaction and power density of the polymer electrolyte fuel cell by under-rib convection, Electrochem. Commun. 13 (2011) 1387–1390.
[18] P. Karthikeyan, R.J. Vasanth, M. Muthukumar, Experimental investigation on uniform and zigzag positioned porous inserts on the rib surface of cathode flow channel for performance enhancement in PEMFC, Int. J. Hydrog. Energy 40 (2015) 4641–4648.
[19] K. Palaniswamy, M. Marappan, V.R. Jothi, Influence of porous carbon inserts on scaling up studies for performance enhancement on PEMFC, Int. J. Hydrog. Energy 41 (2016) 2867–2874.
[20] Y. Cai, T. Yang, P. Sui, J. Xiao, A numerical investigation on the effects of water inlet location and channel surface properties on water transport in PEMFC cathode channels, Int. J. Hydrog. Energy 41 (2016) 16220–16229.
[21] Y. Wang, L. Yue, S. Wang, New design of a cathode flow-field with a sub-channel to improve the polymer electrolyte membrane fuel cell performance, J. Power Sources 344 (2017) 32–38.
[22] A. Turhan, S. Kim, M. Hatzell, M.M. Mench, Impact of channel wall hydrophobicity on through-plane water distribution and flooding behavior in a polymer electrolyte fuel cell, Electrochim. Acta 55 (2010) 2734–2745.
[23] Y. Qin, X. Li, K. Jiao, Q. Du, Y. Yin, Effective removal and transport of water in a PEM fuel cell flow channel having a hydrophilic plate, Appl. Energy 113 (2014) 116–126.
[24] C. Wang, S. Wang, L. Peng, J. Zhang, Z. Shao, J. Huang, C. Sun, M. Ouyang, X. He, Review: recent progress on the key materials and components for proton exchange membrane fuel cells in vehicle applications, Energies 9 (2016) 603.
[25] S.G. Kim, S.J. Lee, A review on experimental evaluation of water management in a polymer electrolyte fuel cell using X-ray imaging technique, J. Power Sources 230 (2013) 101–108.
[26] S.G. Kandlikar, Z. Lu, Thermal management issues in a PEMFC stack—a brief review of current status, Appl. Therm. Eng. 29 (7) (2009) 1276–1280.
[27] W. Dai, H. Wang, X.Z. Yuan, J.J. Martin, D. Yang, J. Qiao, J. Ma, A review on water balance in the membrane electrode assembly of proton exchange membrane fuel cells, Int. J. Hydrog. Energy 34 (23) (December 2009) 9461–9478.
[28] Y. Utaka, I. Hirose, Y. Tasaki, Characteristics of oxygen diffusivity and water distribution by X-ray radiography in microporous media in alternate porous layers of different wettability for moisture control in gas diffusion layer of PEFC, Int. J. Hydrog. Energy 36 (2011) 9128–9138.
[29] R. Koresawa, Y. Utaka, Improvement of oxygen diffusion characteristic in gas diffusion layer with planar-distributed wettability for polymer electrolyte fuel cell, J. Power Sources 271 (2014) 16–24.
[30] Y. Utaka, A. Okabe, Omori, Proposal and examination of method of water removal from gas diffusion layer by applying slanted microgrooves inside gas channel in separator to improve polymer electrolyte fuel cell performance, J. Power Sources 279 (2015) 533–539.
[31] R. Koresawa, Y. Utaka, Water control by employing microgrooves inside gas channel for performance improvement in polymer electrolyte fuel cells, Int. J. Hydrog. Energy 40 (2015) 8172–8181.
[32] Y. Utaka, R. Koresawa, Performance enhancement of polymer electrolyte fuel cells by combining liquid removal mechanisms of a gas diffusion layer with wettability distribution and a gas channel with microgrooves, J. Power

Sources 323 (2016) 37–43.
[33] A. Forner-Cuenca, V. Manzi-Orezzoli, J. Biesdorf, Mario El Kazzi, Daniel Streich, L. Gubler, T.J. Schmidt, P. Boillat, Advanced water management in PEFCs: diffusion layers with patterned wettability I. Synthetic routes, wettability tuning and thermal stability, J. Electrochem. Soc. 163 (13) (2016) F1389–F1398.
[34] A. Forner-Cuenca, J. Biesdorf, A. Lamibrac, V. Manzi-Orezzoli, F.N. Buchi, L. Gubler, T.J. Schmidt, P. Boillat, Advanced water management in PEFCs: II. Measurement of capillary pressure characteristic with neutron and synchrotron imaging, J. Electrochem. Soc. 163 (13) (2016) F1389–F1398.
[35] A. Forner-Cuenca, J. Biesdorf, V. Manzi-Orezzoli, L. Gubler, T.J. Schmidt, P. Boillat, Advanced water management in PEFCs: diffusion layers with patterned wettability III. Operando characterization with neutron imaging, J. Electrochem. Soc. 163 (13) (2016) F1389–F1398.
[36] K. Takaya, T. Araki, Numerical simulation of PEMFC performance considering striped wettability distribution of GDL, ECS Trans. 75 (14) (2016) 563–572.